



High Encapsulation Efficiency of Magnetite Nanoparticles in Hydrophobic Polymer Microcapsules Using Microsuspension Conventional Radical Polymerization

JITTAYA SADCHAIYAPHUM¹, PONGSATHON PHAPUGRANGKUL²,
PREEYPORN CHAIYASAT^{1,3} and AMORN CHAIYASATA^{1,3*}

¹Department of Chemistry, Faculty of Science and Technology, Rajamangala University of Technology Thanyaburi, Klong 6, Thanyaburi, Pathum Thani 12110, Thailand.

²Biodiversity Research Center, Thailand Institute of Scientific and Technological Research, Pathum Thani 12120, Thailand.

³Advanced Materials Design and Development (AMDD) Research Unit, Faculty of Science and Technology, Rajamangala University of Technology Thanyaburi, Klong 6, Thanyaburi, Pathum Thani 12110, Thailand.

*Corresponding author E-mail: a_chaiyasat@mail.rmutt.ac.th

<http://dx.doi.org/10.13005/ojc/350202>

(Received: February 05, 2019; Accepted: April 02, 2019)

ABSTRACT

High encapsulation efficiency of magnetite nanoparticles (MNPs; Fe₃O₄) in microcapsules using PDVB as a hydrophobic polymer shell was successfully achieved by microsuspension conventional radical polymerization (ms CRP). MNPs were initially synthesized by co-precipitation of Fe²⁺/Fe³⁺ in a binary phase. During the nucleation of MNPs in alkaline aqueous solution existing oleic acid (OA), MNPs were coated with OA (MNPs-OA) before moving to the toluene phase with the addition of salt. At OA concentration of 0.3 wt%, most of the nucleated MNPs were hydrophobic and well dispersed in the toluene phase. Using DVB as a monomer for ms CRP, high encapsulation efficiency (92 %EE) of MNPs-OA was obtained, with low free polymer particle formation. By contrast, large amounts of free polymer particles were observed at low %EE (32%) of MNPs. The main driving force for high %EE was obtained by coating the surface of the MNPs by OA which increased hydrophobicity.

Keywords: Microsuspension conventional radical polymerization, Magnetite nanoparticles, Encapsulation efficiency, Microcapsule.

INTRODUCTION

Magnetic particles have been applied

to various fields including magnetic resonance imaging (MRI)^{1,2}, drug delivery^{3,4}, biosensor^{5,6} and separation^{7,8}. Iron oxides as magnetite nanoparticles



(MNPs; Fe_3O_4) are most frequently used because of chemical stability, easy preparation, low cost and fundamental biocompatibility^{1,9,10}. MNPs are commonly prepared by co-precipitation method of Fe^{3+} and Fe^{2+} in basic solution^{11,12}. However, without a surface coating, MNPs with hydrophobic surfaces are unable to maintain colloidal stability when large clusters are formed based on the particle aggregation^{2,4}. Therefore, to overcome this drawback, encapsulation with various hydrophilic polymer chains^{1,9} or polymer shells^{13,14} is preferable. For some applications which require a more durable coating layer, encapsulation of MNPs in a polymer shell as microcapsules is more suitable than coating with small molecules. The microcapsule surface is also easily functionalized using the appropriate functional group for specific applications.

One of the most popular environmentally friendly techniques for microcapsule preparation is microsuspension conventional radical polymerization (ms CRP). High encapsulation efficiency (%EE) is achieved because the polymerization locus is in the monomer droplet where all components such as monomer, initiator and target core materials of the microcapsule are soluble. We have successfully applied ms CRP to encapsulate various kinds of core materials including paraffin wax^{15,16,17,18,19,20,21,22} and fragrance²³. To the best of our knowledge, the main factor affecting encapsulation efficiency results differing polarities of capsule shell and core. Hydrophilic substances diffuse to the interface of the polymerizing particles to form an outer shell, leaving more hydrophobic substances in the core which promote high encapsulation efficiency. However, some hydrophilic monomers are soluble in aqueous phase²⁴, and free polymer particles (without a material core) are formed in competition with the microcapsules^{19,23}. During polymerization, some primary or oligomeric radicals exit from the monomer droplet to the aqueous phase and polymerize with the existing monomer. This phenomenon can be overcome by the adding a hydrophobic chain transfer agent such as iodoform in the monomer phase, named the "RED effect"¹⁸. Therefore, ms CRP is the preferred technique to prepare microcapsules which high encapsulation efficiency that have no free polymer particles using a hydrophobic monomer. Divinylbenzene (DVB) is well-known monomer for encapsulation of hydrophobic cores such as wax^{16,17}. DVB was selected as our model

hydrophobic monomer for MNP encapsulation. However, before the ms CRP technique is applied the MNPs must be well-dispersed in monomer droplets. Oleic acid (OA) was used as a water in oil (W/O) emulsion stabilizer. Previous, researchers have used suspension polymerization to prepare microcapsules containing MNPs or metal oxides^{25,26} but a few have followed a systematic approach to obtain both high encapsulation efficiency and high percentage yield of microcapsules.

Here, preparation of microcapsules containing MNPs was investigated by *ms* CRP using PDVB as a hydrophobic polymer shell. Influence of the hydrophobicity of MNPs on encapsulation efficiency was also examined.

EXPERIMENTAL

Materials

Iron(II) chloride (FeCl_2) (Acros, Geel, Belgium; purity, 97%), iron(III) chloride (FeCl_3) (Aldrich, Wisconsin, USA; purity, 97%), oleic acid (OA) (Aldrich, Wisconsin, USA; purity, 90%), toluene (RCI Labscan, Bangkok, Thailand; purity, 99.5%), ammonia (AppliChem Panreac, Barcelona, Spain; purity, 30%) and sodium chloride (NaCl) (Ajax Finechem, Australia; purity, 99.9%) were used as received. Divinylbenzene (DVB) (Aldrich, Wisconsin, USA; purity, 99%) was purified by passing through a column packed with basic aluminum oxide to remove the inhibitor and kept in a refrigerator until required for use. Benzoyl peroxide (BPO) (Analytical reagents, Merck, Germany) was purified by recrystallization in methanol. Polyvinyl alcohol (PVA) (Aldrich, Wisconsin, USA) with degree of saponification 87-90%, and molecular weight 3.7×10^4 g/mol was used as received.

Synthesis of oleic acid coated-magnetite nanoparticles (MNPs-OA)

MNPs with hydrophobic surfaces were prepared by co-precipitation in a binary aqueous and toluene phase. First, aqueous solutions of FeCl_2 and FeCl_3 were prepared by dissolving 0.50 and 0.87 g, respectively, in 15 ml of water. Then 20 ml of oleic acid solution of the appropriate concentration in toluene was prepared and added into the aqueous solution. Next, the two phases solution was transferred to a round-bottom flask, sealed with a silicone rubber septum and purged with a vacuum/

N₂ cycle five times (finally in N₂). MNPs were then generated as the appearance of a black suspension (mostly in the toluene phase) by a dropwise addition of 5 ml of ammonia (25 wt%) solution under 70°C and 150 cycles/min for 1 hour. To completely separate the black suspension from the aqueous phase, 10 ml of NaCl solution (4 M) was then added. Toluene in the obtained black solution was evaporated. Finally, remaining was washed with water to remove unreacted ammonia. The obtained MNPs coated with oleic acid (MNPs-OA) were expected to disperse in any hydrophobic solvent including a monomer. The recipe for MNP preparation is shown in Table 1.

Table 1: Recipe for preparation of magnetite nanoparticles (MNPs) by co-precipitation with various amounts of oleic acid

Ingredient			
Water phase	FeCl ₂	g (mmol)	0.50 (3.94)
	FeCl ₃	g (mmol)	0.87 (5.39)
	NaCl ^a	mL	10.00
	Water	mL	15.00
	NH ₃ 25%	mL	5.00
Oil phase	Oleic acid ^b	wt%	0.30
	Toluene	mL	20.00

^a NaCl 4 M

^b Oleic acid amount (wt%): 0, 0.1, 0.2, 0.3, 0.4

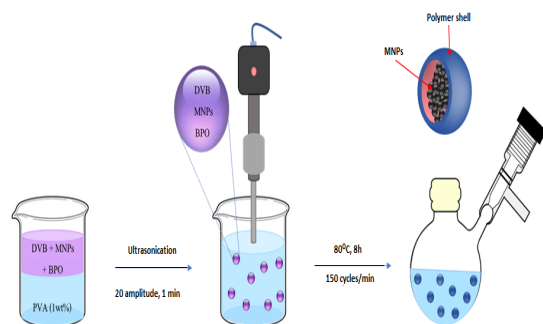


Fig. 1. Schematic diagram for the preparation of PDVB/MNP microcapsules by ms CRP

Table 2: Recipe for preparation of PDVB/MNP microcapsules by ms CRP^a of monomer droplets generated by ultrasonication^b

Ingredient		
DVB	(g)	2.50
MNPs	(g)	2.50
BPO	(g)	0.20
PVA aqueous solution (1 wt%)	(g)	45.00

^a N₂, 80 °C for 8 h,

^b monomer droplets generated by ultrasonication at 20 %amplitude, 1 min

Synthesis of polymer microcapsules

Polymer microcapsule encapsulating MNPs-OA were prepared by ms CRP (Fig. 1) under the conditions listed in Table 2. First, DVB, MNPs-OA and BPO were homogeneously mixed as an oil phase before pouring into a PVA aqueous solution (1 wt%). Thereafter, monomer droplets containing MNPs-OA dispersed in an aqueous phase as an oil-in-water emulsion were produced by applying high shear rate with the ultrasonication of 20% amplitude for 1 minute. The obtained emulsion was subsequently transferred to a round-bottom flask, sealed with a silicone rubber septum and purged with a vacuum/N₂ cycle five times (finally in N₂). The emulsion was finally polymerized at 80°C for 8 h with a shaking rate of 150 cycles/min.

Characterizations

Microcapsule morphology in terms of inner structure and particle surface was observed by an optical microscope (OM) (SK-100 EB and SK-100 ET, Seek Inter Corporation Ltd, Thailand) and a scanning electron microscope (SEM) (JSM-6510, JEOL Ltd, Japan), respectively. Before SEM observation, a drop of polymer suspension was placed onto a nickel SEM stub and dried before coating with gold (A_g). Particle size and morphology of MNPs were determined by dynamic light scattering (DLS, Delsa Nano C, Beckman Coulter, Germany), transmission electron microscopy (TEM, Tecnai 20, Philips, The Netherlands) and X-ray diffraction analysis (XRD) (Rigaku Smartlab-9KW, Japan), respectively. Particle sizes of MNP emulsion (ca 10 wt%) in toluene were measured by the concentration mode at light scattering angle of 165° at room temperature. Before TEM observation, each MNP emulsion was diluted to approximately 50 ppm. Several drops of emulsion were placed on a carbon-coated copper grid which was then dried at room temperature in a desiccator before measurement. Dried MNPs of 10.0 g were packed and measured by XRD at 40 kV, 30 mA and from 5 to 80° 2θ at 25°C. Percent conversion was measured by gravimetry. Polymer emulsions (ca 2.0 g) taken from the reactor were transferred directly into an aluminum cup and weighed. Before drying at 80°C, several drops of hydroquinone solution (1 wt%) as the inhibitor were added. After obtaining constant weight, the monomer conversion was obtained by comparing the weight of dried polymer with that of the original monomer.

MNP contents or loading experiment (L_E) in polymer microcapsules were determined by gravimetry using a compact muffle furnace. Dried microcapsules were burned at 550°C for 10 min to remove coated OA and polymer shell. Residual encapsulated MNPs were weighed and calculated as %LE.

Based on the calculation of theoretical MNP loading in the microcapsules as shown in equation 1, encapsulation efficiency in terms of percent encapsulation (%EE) was obtained from equation 2.

$$\%L_{th} = \frac{W_{MNP_s}}{W_{MNP_s} + [(\%Conv - \%F_p)/100] \times W_M} \times 100 \quad (1)$$

$$\%E = \frac{\%L_E}{\%L_{th}} \times 100 \quad (2)$$

Where W_{MNP_s} and W_M are the weights of MNPs and monomer from the recipe, respectively, %Conv and % F_p are the percent of monomer conversion and free polymer particles, respectively, %EE is the percent encapsulation, % L_E is the experiment loading (wt%) and % L_{th} is the theoretical percentage loading (wt%).

RESULTS AND DISCUSSION

Synthesis of oleic acid-coated magnetite nanoparticles (MNPs-OA)

To encapsulate MNPs inside polymer capsules prepared by ms CRP where polymerization locus is in the monomer droplet dispersed in an aqueous medium, the MNP surfaces required hydrophobicity. Therefore, before ms CRP, MNPs were prepared by coating with a hydrophobic substance. OA has a low hydrophilic-lipophilic balance (HLB) value of 1 and is often used as a water in oil (W/O) emulsion emulsifier. It also used for metal oxide particle surface coating^{27,28} to increase hydrophobicity. To prepare MNPs in a binary phase of both hydrophilic (aqueous) and hydrophobic (toluene containing OA) phases, MNPs as Fe_3O_4 nanoparticles were first nucleated in an aqueous medium by co-precipitation of Fe^{2+} and Fe^{3+} under alkaline condition and mild stirring. Thereafter, nucleated MNPs moved up to the toluene phase with presentation of salt. OA has a carboxyl group and some may diffuse to the aqueous phase, although previously added in the toluene phase. Nucleated MNPs were then coated by OA via both chemical bonding and hydrogen bonding as MNPs-OA. MNPs

were first covalent-bonded with OA by the reaction between hydroxyl and carboxyl groups of MNP surface and OA chain, respectively. The second layer was formed via physical adsorption and hydrogen bonding when a larger amount of OA was presented and accorded with coating of OA onto the surface of other metal oxides as $ZnAl_2O_4$ ²⁷ and CdS²⁸ nanoparticles. After the addition of salt into the binary phase, water solubility of OA was dramatically reduced based on the salting-out effect and MNPs-OA then moved up into the toluene phase. A possible schematic of MNPs-OA preparation is shown in Figure 2.

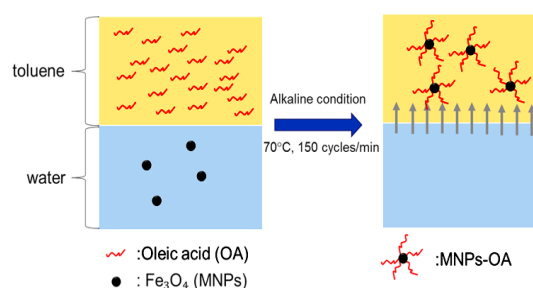


Fig. 2. Schematic diagram for preparation of MNPs-OA by co-precipitation in a binary phase

Influence of OA amount on the hydrophobicity of MNPs-OA surface was then investigated. Various amounts of OA (0-0.4 wt% in toluene) were added into the toluene phase. As seen in Fig. 3, all nucleated MNPs either precipitated or dispersed in the aqueous medium in the absence of OA (Fig. 3a). In the toluene phase, amount of MNPs-OA moving into the toluene phase increased with OA content. All MNPs-OA dispersed only in the toluene phase and transparent bottom (aqueous) phase was observed at 0.3 wt% OA or higher (Fig. 3c and d). In addition, %yield of MNPs reached maximum value as 98 (SD; 1.5)% and 98 (SD; 2.4)% for 0.3 and 0.4 wt% of OA, respectively. Therefore, 0.3 wt% of OA was selected for preparation of MNPs-OA for further experiments.

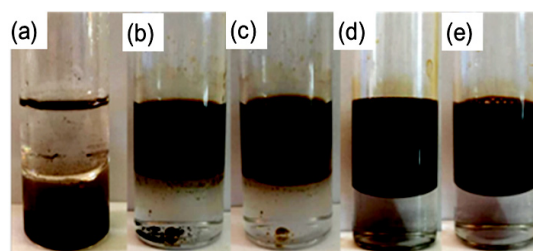


Fig. 3. Photos of MNPs-OA prepared by co-precipitation in a binary phase with various amounts of OA (wt%): (a) 0, (b) 0.1, (c) 0.2, (d) 0.3 and (e) 0.4

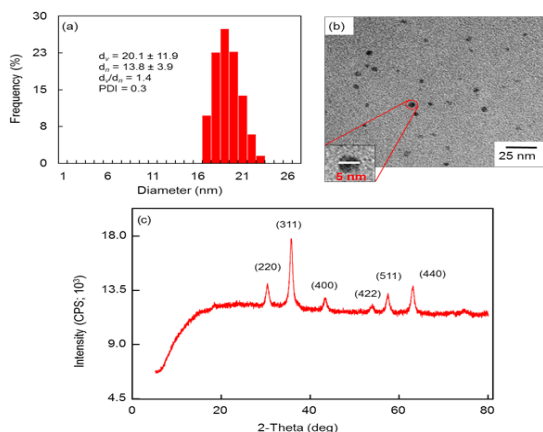


Fig. 4. DLS histogram (a), TEM photo (b) and XRD pattern (c) of MNPs prepared by co-precipitation in a binary phase using OA of 0.3 wt%

Characterization of synthesized MNPs-OA is shown in Fig. 4. Particle size of MNPs-OA measured by DLS (Fig. 4a) was 14 nm (number average particle size) with a narrow particle size distribution (PDI; 0.3). This indicated that OA effectively stabilized MNPs dispersed in the toluene phase. Moreover, spherical MNPs-OA average size of 5 nm was observed by TEM (Fig. 4b). The smaller size observed by TEM was due to collapse of the OA chains onto MNP surface in the dried state of TEM measurement. In addition, XRD pattern of the obtained MNPs-OA is shown in Fig. 4c. Main diffraction peaks were observed at 30°, 35°, 44°, 53°, 56° and 62° accounting for crystal planes of (220), (311), (400), (422) and (511), respectively, which corresponded to Fe_3O_4 phases^{9,29}.

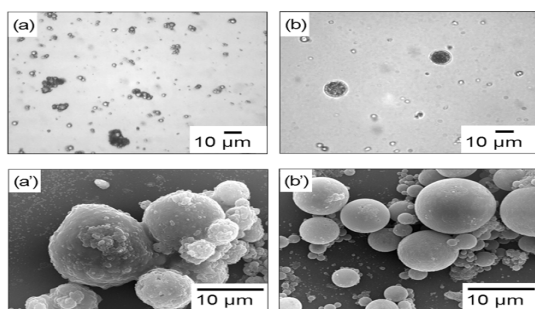


Fig. 5. Optical (a and b) and SEM micrographs (a' and b') of PDVB/MNP microcapsules prepared by ms CRP using MNPs without (a and a') and with (b and b') coating of OA

Synthesis of polymer microcapsules

Here, polymer microcapsule encapsulating MNPs-OA were prepared by ms CRP. Monomer

droplets containing initiator and MNPs-OA were dispersed in an aqueous medium containing PVA surfactant. Colloidal stability of the monomer droplets was maintained by adsorbed surfactant onto the monomer droplet surfaces based on steric repulsion of PVA chains. In ms CRP, some primary or oligomeric radicals exited from the monomer droplet into the aqueous medium during polymerization. Thereafter, free polymer particles were nucleated when the monomer existed in an aqueous medium. To depress this phenomenon, DVB, a hydrophobic monomer which is only slightly soluble in water was used. However, because of high hydrophobicity of the polymer shell, the formed polymer chains had difficulty diffusing to the polymerizing particle surface to envelope the MNPs since the surface was less hydrophobic.

Therefore, the influence of prepared MNPs with (0.3 wt%) and without a coating of OA on encapsulation efficiency was investigated. The obtained PDVB/MNPs particles were observed using both OM (Fig. 5a and b) and SEM (Fig. 5a' and b'). Nonspherical particles were clearly observed with OM (Fig. 5a) in the case of MNPs without OA. This may be due to the less hydrophobic MNPs which either move to or out of the polymerizing particle surface. This may also disturb the stabilization of PVA where most of the obtained PDVB/MNPs coalesced. This phenomenon accorded with SEM measurement where an irregular PDVB/MNP surface was observed (Fig. 5a'). By contrast, using MNPs-OA resulted in spherical PDVB/MNPs-OA microcapsules observed under OM (Fig. 5b). The more hydrophobic surface of MNPs-OA was well-dispersed in monomer droplets and polymerizing particles. This result agreed with the SEM photo (Fig. 5b') where spherical PDVB/MNPs-OA microcapsules with smooth outer surfaces were observed.

Both PDVB/MNPs (Fig. 6a) and PDVB/MNPs-OA (Fig. 6b) microcapsules gave similar brown suspensions. After a magnetic field was applied, most PDVB/MNPs-OA microcapsules (Fig. 6b') were magnetized and moved to the bottle wall, leaving a transparent aqueous medium. By contrast, free PDVB particles remained dispersed in the aqueous medium as a milky suspension (Fig. 6a') in the case of PDVB/MNPs, although some microcapsules were magnetized. This supported our

assumption that during polymerization, MNPs without coating exited the monomer/polymerizing particles.

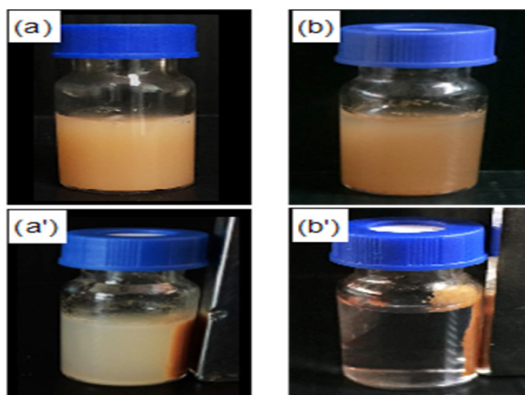


Fig. 6. Suspension photos of PDVB/MNPs (a and a') and PDVB/MNPs-OA (b and b') microcapsules prepared by ms CRP before (a-b) and after (a'-b') applying a magnetic field

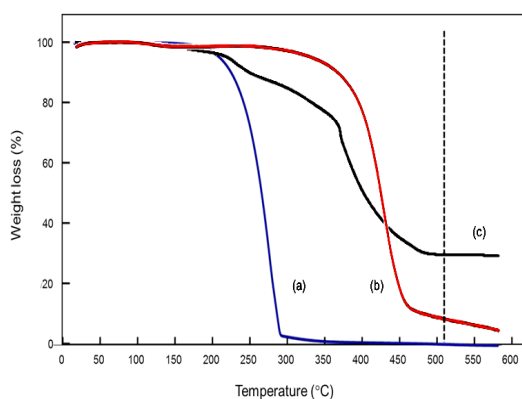


Fig. 7. TGA thermograms of OA (a), PDVB (b) and PDVB/MNPs-OA (c)

TGA thermograms of OA, PDVB and PDVB/MNPs-OA are shown in Fig. 7. Decomposition temperature ranges of OA (Fig. 7a) and PDVB (Fig. 7b) were about 150-300°C and 330-550°C, respectively. In the case of PDVB/MNPs-OA microcapsules (Fig. 7c), the first two steps corresponded to decomposition temperature ranges of OA and PDVB, whereas weight loss seemed constant after about 520°C which might reflect the remaining MNPs. Therefore, to measure the % L_E of MNPs, coating components as OA and PDVB shell were burned above their decomposition temperatures

(550°C) to leave a residual component as MNPs. Percent L_E was then measured as shown in Table 3. Percent L_E of MNPs-OA was over three times the value of uncoated MNPs. In addition, based on equation 2, encapsulation efficiency (%EE) of MNPs-OA was about 92%. These results concurred with previous experiments of OM and SEM observation and indicated that the presence of OA on the MNPs surface plays an important role for encapsulation of MNPs in hydrophobic polymer microcapsules.

Table 3: Percent loading and encapsulation of MNPs with and without coating of OA in microcapsules prepared by ms CRP

Microcapsule	Percent loading (wt%)		Percent EE ^b (wt%)
	L_{in}^a	$L_E (\pm SD)^c$	
PDVB/MNPs	22	7 ± 2.2	32
PDVB/MNPs-OA	26	24 ± 3.1	92

^a calculated using equation 1

^b calculated using equation 2

CONCLUSION

High encapsulation efficiency of MNPs by ms CRP using a hydrophobic polymer shell was successfully achieved. Hydrophobicity of the MNP surface was the main factor for retention of MNPs inside the hydrophobic polymer shell. Based on both chemical bonding and physical adsorption of OA onto the MNPs surface, MNPs-OA effectively remained inside the microcapsule. This finding is not only appropriate to produce PDVB/MNPs-OA microcapsules but may also be useful for preparation of microcapsules containing other metal oxide particles.

ACKNOWLEDGEMENT

This research was partially supported by the "Partnership Program in Production of Graduates in Master and Doctoral Degrees Between the Thailand Institute of Scientific and Technological Research (TISTR) and Educational institutions", Thailand Institute of Scientific and Technological Research (given to J.S.).

Conflict of Interest

The authors declare that they have no conflict of interest.

REFERENCES

- Soares, P.I.P.; Laia, C.A.T.; Carvalho, A.; Pereira, L.C.J.; Coutinho, J.T.; Ferreira, I.M.M.; Novo, C.M.M. and Borges, J.P. *Applied Surface Science.*, **2016**, *383*, 240-247.

2. Cheng, F.-Y.; Su, C.-H.; Yang, Y.-S.; Yeh, C.-S.; Tsai, C.-Y.; Wu, C.-L.; Wu, M.-T. and Shieh, D.-B. *Biomaterials.*, **2005**, *26*(7), 729-738.
3. Tan, S.T.; Wendorff, J.H.; Pietzonka, C.; Jia, Z.H. and Wang, G.Q. *ChemPhysChem.*, **2005**, *6*(8), 1461-1465.
4. Hu, J.; Qian, Y.; Wang, X.; Liu, T. and Liu, S. *Langmuir.*, **2012**, *28*(4), 2073-2082.
5. Jie, G.; Wang, L.; Yuan, J. and Zhang, S. *Analytical Chemistry.*, **2011**, *83*(10), 3873-3880.
6. Wang, J.; Munir, A.; Zhu, Z. and Zhou, H.S. *Analytical Chemistry.*, **2010**, *82*(16), 6782-6789.
7. Bruce, I.J. and Sen, T. *Langmuir.*, **2005**, *21*(15), 7029-7035.
8. Bao, J.; Chen, W.; Liu, T.; Zhu, Y.; Jin, P.; Wang, L.; Liu, J.; Wei, Y. and Li, Y. *ACS Nano.*, **2007**, *1*(4), 293-298.
9. Shete, P.B.; Patil, R.M.; Tiwale, B.M. and Pawar, S.H. *Journal of Magnetism and Magnetic Materials.*, **2015**, *377*, 406-410.
10. Esmaeili, E.; Ghiass, M.A.; Vossoughi, M. and Soleimani, M. *Scientific Reports.*, **2017**, *7*(1), 194.
11. Mahdavi, M.; Ahmad, M.B.; Haron, M.J.; Namvar, F.; Nadi, B.; Rahman, M.Z.A. and Amin, J. *Molecules.*, **2013**, *18*(7), 7533.
12. Barrow, M.; Taylor, A.; Murray, P.; Rosseinsky, M.J. and Adams, D.J. *Chemical Society Reviews.*, **2015**, *44*(19), 6733-6748.
13. Xu, S.; Yang, F.; Zhou, X.; Zhuang, Y.; Liu, B.; Mu, Y.; Wang, X.; Shen, H.; Zhi, G. and Wu, D. *ACS Applied Materials & Interfaces.*, **2015**, *7*(36), 20460-20468.
14. Omi, A.; Kanetaka, Y.; Shimamori, A.; Supsakulchai, M.; Nagai, G.-H. and Ma, S. *Journal of Microencapsulation.*, **2001**, *18*(6), 749-765.
15. Chaiyasat, A.; Namwong, S.; Uapipatanakul, B.; Sajomsang, W. and Chaiyasat, P. *International Journal of GEOMATE.*, **2018**, *14*(45), 91-98.
16. Namwong, S.; Islam, M.Z.; Noppalit, S.; Tangboriboonrat, P.; Chaiyasat, P. and Chaiyasat, A. *Journal of Macromolecular Science, Part A: Pure and Applied Chemistry.*, **2016**, *53*(1), 11-17.
17. Namwong, S.; Noppalit, S.; Okubo, M.; Moonmungmee, S.; Chaiyasat, P. and Chaiyasat, A. *Polymer - Plastics Technology and Engineering.*, **2015**, *54*(8), 779-785.
18. Chaiyasat, P.; Noppalit, S.; Okubo, M. and Chaiyasat, A. *Solar Energy Materials and Solar Cells.*, **2016**, *157*, 996-1003.
19. Chaiyasat, P.; Noppalit, S.; Okubo, M. and Chaiyasat, A. *Physical Chemistry Chemical Physics.*, **2015**, *17*(2), 1053-1059.
20. Chaiyasat, P.; Islam, M.Z. and Chaiyasat, A. *RSC Advances.*, **2013**, *3*(26), 10202-10207.
21. Supatimusro, D.; Promdsorn, S.; Thipsit, S.; Boontung, W.; Chaiyasat, P. and Chaiyasat, A. *Polymer - Plastics Technology and Engineering.*, **2012**, *51*(11), 1167-1172.
22. Chaiyasat, P.; Chaiyasat, A.; Boontung, W.; Promdsorn, S. and Thipsit, S. *Materials Sciences and Applications.*, **2011**, *2*(8), 1007-1013.
23. Pansuwan, J. and Chaiyasat, A. *Polymer International.*, **2017**, *66*(12), 1921-1927.
24. Chaiyasat, P.; Namwong, S.; Okubo, M. and Chaiyasat, A. *RSC Advances.*, **2016**, *6*(97), 95062-95066.
25. Dong, Y.Z.; Han, W.J. and Choi, H.J. *Polymers.*, **2018**, *10*(3), 299.
26. Ahmad, H.; Sharafat, M.K.; Alam, M.A.; Rahman, M.M.; Tauer, K.; Minami, H.; Sultana, M.S.; Das, B.K. and Shabnam, R. *Macromolecular Research.*, **2017**, *25*(7), 671-679.
27. Song, X.; Zheng, S.; Zhang, J.; Li, W.; Chen, Q. and Cao, B. *Materials Research Bulletin.*, **2012**, *47*(12), 4305-4310.
28. Zheng, X.; Weng, J. and Hu, B. *Materials Science in Semiconductor Processing.*, **2010**, *13*(3), 217-220.
29. Velusamy, P.; Chia-Hung, S.; Shritama, A.; Kumar, G.V.; Jeyanthi, V. and Pandian, K. *Journal of the Taiwan Institute of Chemical Engineers.*, **2016**, *59*, 450-456.